



Photoexcitation and -ionization in helium: Zero-kinetic-energy spectroscopy

Citation

Fan, Zhuang, H. R. Sadeghpour, and A. Dalgarno. 1994. "Photoexcitation and -Ionization in Helium: Zero-Kinetic-Energy Spectroscopy." *Physical Review A* 50 (4): 3174–76. <https://doi.org/10.1103/physreva.50.3174>.

Permanent link

<http://nrs.harvard.edu/urn-3:HUL.InstRepos:41417403>

Terms of Use

This article was downloaded from Harvard University's DASH repository, and is made available under the terms and conditions applicable to Other Posted Material, as set forth at <http://nrs.harvard.edu/urn-3:HUL.InstRepos:dash.current.terms-of-use#LAA>

Share Your Story

The Harvard community has made this article openly available. Please share how this access benefits you. [Submit a story](#).

[Accessibility](#)

Photoexcitation and -ionization in helium: Zero-kinetic-energy spectroscopy

Zhuang Fan,* H. R. Sadeghpour, and A. Dalgarno

Harvard-Smithsonian Center for Astrophysics, 60 Garden Street, Cambridge, Massachusetts 02138

(Received 31 May 1994)

The cross sections for double and single photoexcitation and -ionization of helium are calculated in the acceleration gauge assuming a totally asymmetric energy and angular momentum partitioning between two electrons. The electron-electron correlation is taken into account in the ground-state wave function. By extrapolating single-ionization differential oscillator strengths to $n \rightarrow \infty$, where n is the excited He^+ principal quantum number, an estimate of the double-ionization cross sections is obtained. Comparison with other calculations is made.

PACS number(s): 32.80.Fb, 32.30.Rj, 32.70.Cs, 33.60.Fy

I. INTRODUCTION

The double photoionization of helium has received considerable attention because of the central role played by the electron-electron correlation in the ejection of two electrons by the absorption of a single photon. Electron-electron correlation is also an essential feature in the process of simultaneous excitation and ionization in which one electron is ejected and the residual ion is left in an excited state. The high-frequency limits of the excitation-ionization process have been calculated [1–3], but no results have appeared on the cross sections at other energies. The cross sections for photoionization leaving He^+ in a high Rydberg level are valuable also because they can be extrapolated to the double-escape threshold for the ejection of a very slow (zero-energy) photoelectron and a fast photoelectron which takes up all the available energy.

We use an uncorrelated symmetrized product of hydrogenic wave functions for the residual ion states of $\text{He}^+(ns)$ and an energy-normalized Coulomb wave function for the photoelectron to calculate single-photoionization continuum oscillator strengths for producing excited $\text{He}^+(n)$ states. The results for excitation ionization of helium by photons are shown in Sec. II. Comparison with the asymptotic theory is also presented.

II. CALCULATIONS

The differential oscillator strength for the excitation ionization process

$$h\nu + \text{He} \rightarrow \text{He}^+(ns) + e^- \quad (1)$$

is given in the acceleration formulation by

$$\frac{df_n^+}{d\varepsilon} = \frac{2Z^2}{\omega^3} \left| \left\langle \psi_n(\mathbf{r}_1, \mathbf{r}_2) \left| \frac{\mathbf{r}_1}{r_1^3} + \frac{\mathbf{r}_2}{r_2^3} \right| \Psi(\mathbf{r}_1, \mathbf{r}_2) \right\rangle \right|^2, \quad (2)$$

where \mathbf{r}_1 and \mathbf{r}_2 are the position vectors of the two electrons, $\Psi(\mathbf{r}_1, \mathbf{r}_2)$ is the ground-state wave function of helium, $\psi_n(\mathbf{r}_1, \mathbf{r}_2)$ is the final-state wave function, ω is the photon frequency in atomic units, Z is the nuclear charge, and ε is the energy of the ejected photoelectron, i.e., $\varepsilon = \omega + E_0 - 2/n^2$, with E_0 the ground-state energy.

At large values of ω , $\varepsilon \rightarrow \omega$, and Eq. (2) becomes [4]

$$\frac{df_n^+}{d\varepsilon} = C(ns)(2\varepsilon)^{-7/2}, \quad (3a)$$

where

$$C(ns) = \frac{512\pi Z^2}{3} |\langle \Psi(\mathbf{r}_1, \mathbf{r}_2) | \delta(r_2) | u_{ns}(r_1) \rangle|^2, \quad (3b)$$

in which $u_{ns}(r)$ is the regular radial wave function of the ns state of He^+ .

We have evaluated Eq. (2) using for the ground-state wave function a 21-configuration Hartree-Fock wave function of Froese Fischer [5] and for the final-state wave function an uncorrelated representation consisting of an antisymmetric product of a helium ion wave function for the bound electron and a screened Coulomb continuum function for the ejected electron. This choice leads in the acceleration gauge to cross sections that are accurate in the limit of high frequencies. Differential oscillator strengths $df_n^+/d\varepsilon$ for exciting $\text{He}^+(ns)$ levels up to $n = 16$ were calculated.

Figure 1 shows our predicted differential oscillator strengths in the form of $(2\varepsilon)^{7/2}(df_n^+/d\varepsilon)$. The differential oscillator strengths behave similarly with energy for the different excited states ns and slowly approach the asymptotic form given by Eq. (3b) [6].

A comparison of the coefficients $C(ns)$ obtained for the high-frequency limits of Eq. (2) with those obtained by evaluating Eq. (3b) is given in Table I. The differences of about 14% are a reflection of the choice of the initial-state wave function and its behavior near the nucleus. The ratios of the coefficients agree closely, suggesting that our calculated cross sections can be improved in accuracy simply by multiplying them by this constant ratio of 1.14.

The limiting values of $n^3(df_n^+/d\varepsilon)$ at the spectral head,

*Present address: Joint Institute for Laboratory Astrophysics, University of Colorado, Boulder, CO 80309.

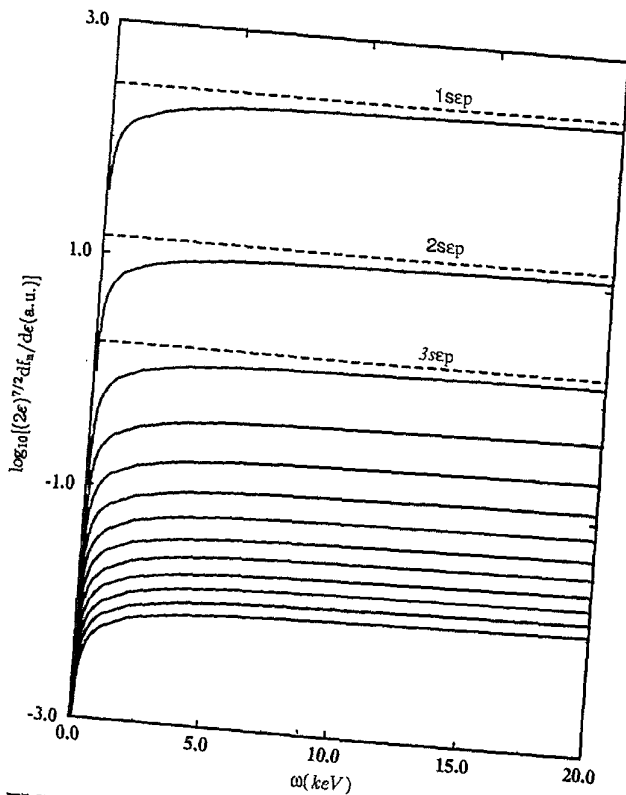


FIG. 1. Differential oscillator strengths in a.u. for exciting $\text{He}^+(ns)$ levels as a function of the photon frequency. The oscillator strengths are scaled by an energy prefactor such that the high-energy tails converge to the constants, $C(ns)$ in Eq. (3a), shown as dashed lines.

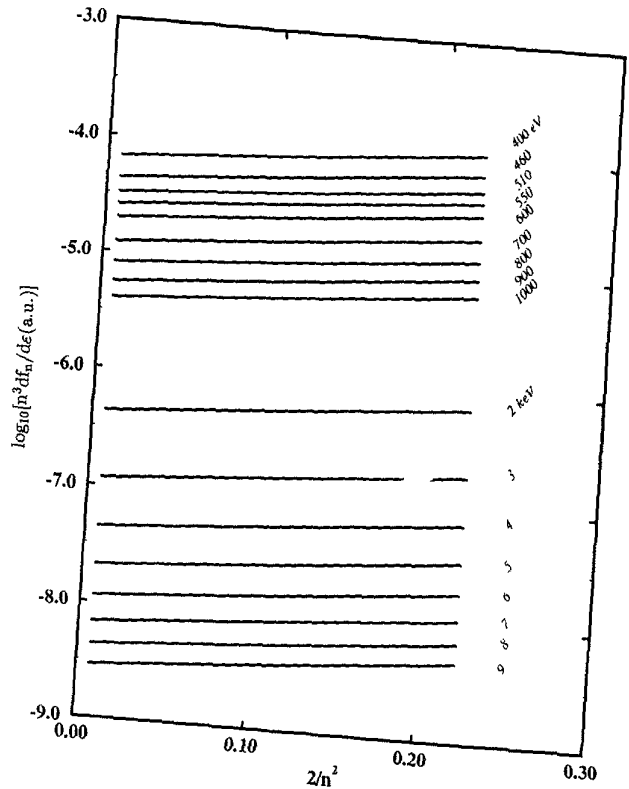


FIG. 2. Differential oscillator strengths in a.u., scaled by n^3 , at several photon energies as a function of energy below threshold. The limiting values at $n = \infty$ are the threshold continuum doubly differential oscillator strengths corresponding to the ejection of one ZKE electron and the other with energy $E_0 + \omega$.

as n tends to infinity, are the threshold continuum doubly differential oscillator strengths $d^2f/d\epsilon d\epsilon'$ corresponding to the ejection of one zero-kinetic-energy (ZKE) electron $\epsilon' = 0$ and the other with energy $\epsilon = \omega + E_0$. For the present calculation E_0 from the multiconfiguration Hartree-Fock (MCHF) calculation is -2.9034761 a.u.

Figure 2 illustrates the behavior of $n^3(df_n/d\epsilon)$ as a function of $2/n^2$ for several energies. At the spectral heads, $2/n^2 = 0$, the functions are linearly decreasing functions. We can evaluate the differential cross section

$$\left. \frac{d\sigma^{2+}(\omega)}{d\epsilon'} \right|_{\epsilon'=0} = \frac{2\pi^2}{137} \left. \frac{d^2f}{d\epsilon d\epsilon'} \right|_{\epsilon'=0},$$

where the fast photoelectron has a definite energy ϵ . The threshold cross sections are shown in Fig. 3. The points are from a direct calculation of double-photoelectron ejection from helium by Kornberg and Miraglia [6] at

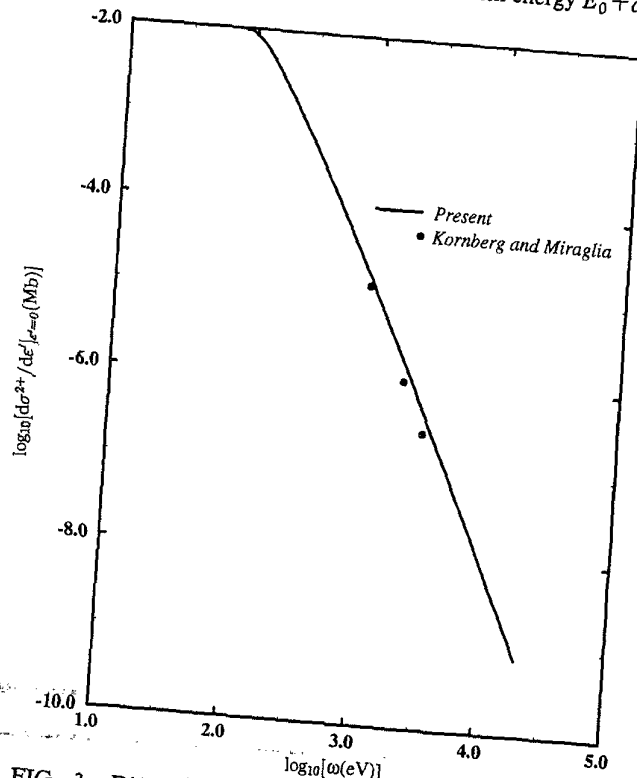


FIG. 3. Differential DPI cross section in megabarns at threshold. The points are from the recent calculations of Ref. [6] at photoelectron energies just near the threshold. The ion energy for the photoelectron is $\epsilon = \omega + E_0$.

TABLE I. Comparison of the asymptotically exact photoionization coefficients and the high-frequency limits of present theory.

| Coefficient | Present | Eq. (3b) | Ratio |
|-------------|---------|----------|-------|
| $C(1s)$ | 253.980 | 287.326 | 1.13 |
| $C(2s)$ | 12.200 | 13.754 | 1.13 |
| $C(3s)$ | 1.500 | 1.711 | 1.14 |
| $C(4s)$ | 0.496 | 0.567 | 1.14 |

photoelectron energies near threshold, using an approximate representation of the two-electron continuum wave function.

Since the doubly differential oscillator strengths $df^2/d\epsilon d\epsilon'$ are continuous across the threshold, we extrapolate the linear behavior to above threshold as

$$\frac{d\sigma^{2+}(\omega)}{d\epsilon'} \sim \frac{d\sigma^{2+}}{d\epsilon'} \Big|_{\epsilon'=0} + a\epsilon', \quad (4)$$

where $d\sigma^{2+}/d\epsilon'|_{\epsilon'=0}$ is known from Fig. 3 and the parameter a is obtained by fitting to the curves of Fig. 2. Since the phase space for photoabsorption becomes localized at the extremes of high momenta, we obtain an estimate of the double-photoionization (DPI) cross section from the expression

$$\sigma^{2+}(\omega) = 2 \int_0^{\epsilon'_0} \frac{d\sigma^{2+}(\omega)}{d\epsilon'} d\epsilon', \quad (5)$$

where the upper limit makes the differential cross section in Eq. (4) zero and the factor 2 is due to the ejection of two electrons. The result of this approximation is shown in Fig. 4, where it is compared with the DPI cross sections of Hino *et al.* [7] and Kornberg and Miraglia [8], which agree closely with the results of the correlated final-state calculations of Hino [9]. The simple approximation Eq. (5) is very successful at energies above 3 KeV. We emphasize that, although the results in Fig. 3 for the differential cross section at threshold are exact within the framework of the present method, Fig. 4 is an approximation whose accuracy is improved with increasing frequency. Thus the low-energy region of our calculations in Fig. 4 must be viewed with caution as the linear approximation used to obtain the results of Fig. 4 is no longer valid.

III. CONCLUSION

In summary, we have shown that using a simple extrapolation technique which exploits the continuity of differential oscillator strength across individual $\text{He}^+(n)$ thresholds, the two-electron ejection by a single photon of high energy is driven by the correlation of two electrons in the ground state. This work is a further numeri-

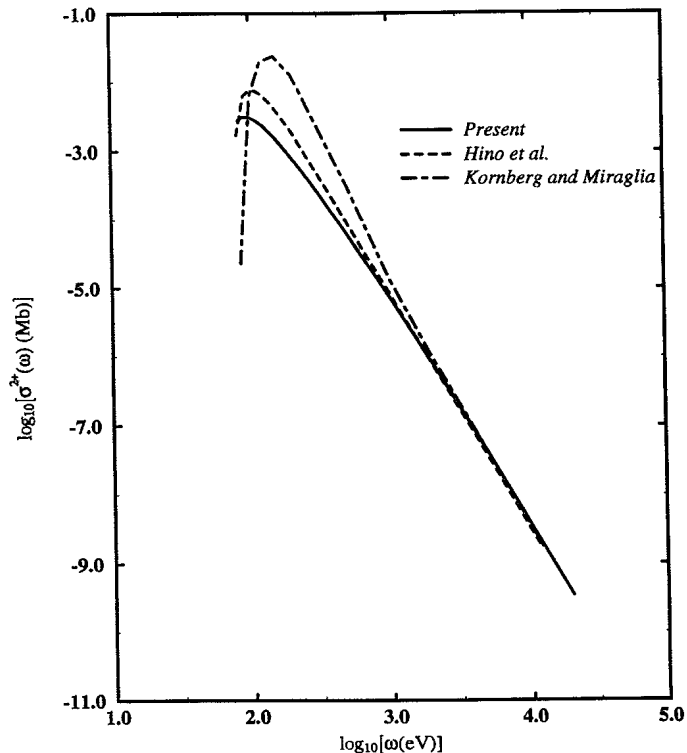


FIG. 4. Total DPI cross sections in megabarns as a function of photon frequency. The present results are from the linear approximation of Eq. (5) and the dashed and dot-dashed curves are from Refs. [7] and [8], respectively.

cal confirmation [7,8] of the predictions of Dalgarno and Sadeghpour [4], who argued that a proper choice of the form of the electric dipole operator would lead to the correct asymptotic DPI ratio.

ACKNOWLEDGMENTS

This work was supported by the U.S. Department of Energy, Division of Chemical Sciences, Office of Basic Energy Sciences, Office of Energy Research. We thank C. Fischer for access to her MCHF wave function.

- [1] P. K. Kabir and E. E. Salpeter, *Phys. Rev.* **108**, 1256 (1957).
- [2] A. Dalgarno and A. L. Stewart, *Proc. Phys. Soc. London* **76**, 49 (1960).
- [3] T. Aberg, *Phys. Rev. A* **2**, 1726 (1970).
- [4] A. Dalgarno and H. R. Sadeghpour, *Phys. Rev. A* **46**, R3591 (1992).
- [5] C. Froese Fischer (private communication).

- [6] M. A. Kornberg and J. E. Miraglia (private communication).
- [7] K. Hino, T. Ishihara, F. Shimizu, N. Toshima, and J. H. McGuire, *Phys. Rev. A* **48**, 1271 (1993).
- [8] M. A. Kornberg and J. E. Miraglia, *Phys. Rev. A* **48**, 3714 (1993).
- [9] K. Hino, *Phys. Rev. A* **47**, 4845 (1993).